Shape and Material from Sound

Zhoutong Zhang
MIT

Qiujia Li
University of Cambridge

Zhengjia Huang
ShanghaiTech University

Jiajun Wu
MIT

Joshua B. Tenenbaum
MIT

William T. Freeman
MIT, Google Research

Abstract

What can we infer from hearing an object falling onto the ground? Based on knowledge of the physical world, humans are able to infer rich information from such limited data: the rough shape of the object, its material, the height of the fall, etc. In this paper, we aim to approximate such competency. We first mimic the human knowledge about the physical world using a fast physics-based generative model. Then, we present an analysis-by-synthesis approach to infer properties of the falling object. We further approximate human past experience by directly mapping audio to object properties using deep learning with self-supervision. We evaluate our method through behavioral studies, where we compare human predictions with ours on inferring object shape, material and initial height of falling. Results show that our method achieves near-human performance, without any annotations. We further test our model using real world data, illustrating its potential in inference from real world data.

1 Introduction

Given a short audio clip of interacting objects, humans, even young children, can recover rich information about materials, surface smoothness, and the quantity of objects involved [Zwicker and Fastl, 2013, Kunkler-Peck and Turvey, 2000, Siegel et al., 2014]. How does our cognitive system recover so much content from the audio clip? What is the role of past experience in understanding auditory inputs?

For physical scene understanding from visual input, recent behavioral and computational studies suggest that human judgments can be well explained as approximate, probabilistic simulations of a mental physics engine [Battaglia et al., 2013, Sanborn et al., 2013]. These studies suggest that the brain encodes rich but noisy knowledge of physical properties of objects and basic laws of physical interactions between objects. To understand, reason, and predict about a physical scene, humans seem to rely on simulations from this mental physics engine.

In this paper, we develop a computational system to interpret audio clips of falling objects, inspired by the idea that humans may use a physics engine as part of a generative model to understand the physical world. The first component of our generative model is the representation of a rigid object, which includes its 3D geometric shape, position in space, and its physical properties including mass, Young's modulus, Rayleigh damping coefficients, and restitution. All of these object attributes are treated as latent variables in our model, which we aim to infer from auditory inputs.

The second part includes an efficient physics-based audio synthesis engine. Given the initial conditions and properties of an object, which serves as the hypothesis for our generative model, the engine first simulates the rigid body motion of the object and generate the object's trajectory with corresponding collision profile under rigid body physics. Then the object's trajectory and collision profile, along with its pre-computed sound statistics, are used to generate the sound of this entire physical process.

31st Conference on Neural Information Processing Systems (NIPS 2017), Long Beach, CA, USA.

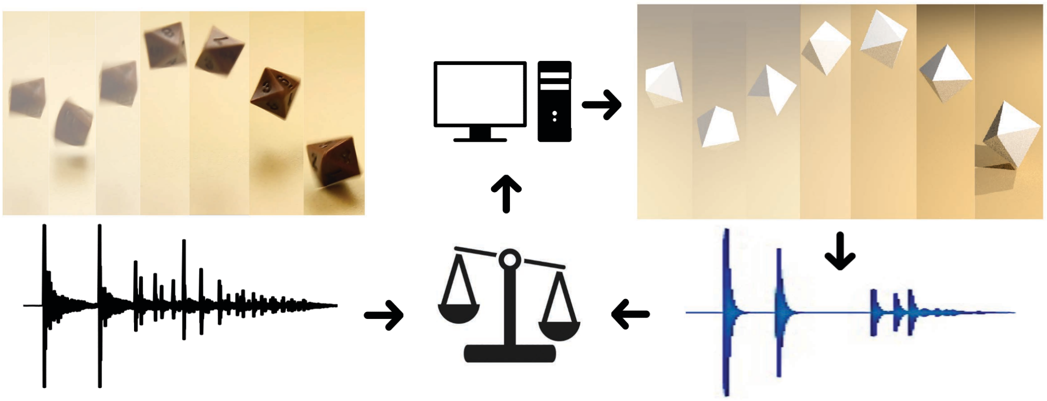

Figure 1: Given an audio of a single object falling, we utilize our generative model to infer latent variables that could best reproduce the sound.

With such efficient forward models, it is possible for us to infer the prescribed latent variables in an analysis-by-synthesis style. In short, given an audio clip, we aim to find a set of latent variables that best reproduce it. One challenge in this goal is to design a likelihood function that measures the perceptual distance between two sounds. To address this challenge, we utilize the observation that a simple feature space, such as spectrogram, can be effective if the degrees of freedom for latent variables are restricted. This observation allows us to infer latent variables via methods like Gibbs sampling, where we can only focus on approximating the conditional probability of a single variable given the others.

To further accelerate our inference procedure, we incorporate past experience via a supervised learning system that uses unlabeled data with inferred labels. To this end, we propose a self-supervised learning algorithm inspired by the wake/sleep phases in Helmholtz machines [Dayan et al., 1995]. A deep neural network is trained as the recognition model (*i.e.*, sleep cycle), where the labels are generated using our inference algorithm. Then, for any future audio clip, the output of the recognition model can be used as a good initialization, accelerating the inference procedure.

We evaluate our models on a range of perception tasks: inferring object shape, material and initial height from the sound. We also collect human responses for each of these tasks and compare them with model estimates. Our results indicate that humans are quite successful in these tasks; our model not only closely matches human successes, but also makes similar errors as humans do. Due to the hardness of acquiring quality audio data with rich labels, we use synthetic data to evaluate our models in above tasks. To prove our model is capable of such inference tasks given real world audio, we tested our model using real captured data under constraint settings.

Our work makes three contributions. First, we propose a novel model for estimating physical properties of objects from auditory inputs by incorporating the feedback of a physics engine and an audio engine into the inference process. Second, we train a deep learning based recognition model that leads to efficient inference in the generative model. Third, we test our model and compare it to humans on a variety of judgment tasks, and demonstrate the correlation between human responses and model estimates.

2 Related Work

Human visual and auditory perception In the field of auditory perception or psychoacoustics, researchers have explored how humans can infer object properties including shape, material, size from audio in the past decades [Zwicker and Fastl, 2013, Kunkler-Peck and Turvey, 2000, Rocchesso and Fontana, 2003, Klatzky et al., 2000, Siegel et al., 2014]. Recently, McDermott et al. [2013] proposed compact sound representations that capture semantic information and are informative of human auditory perception.

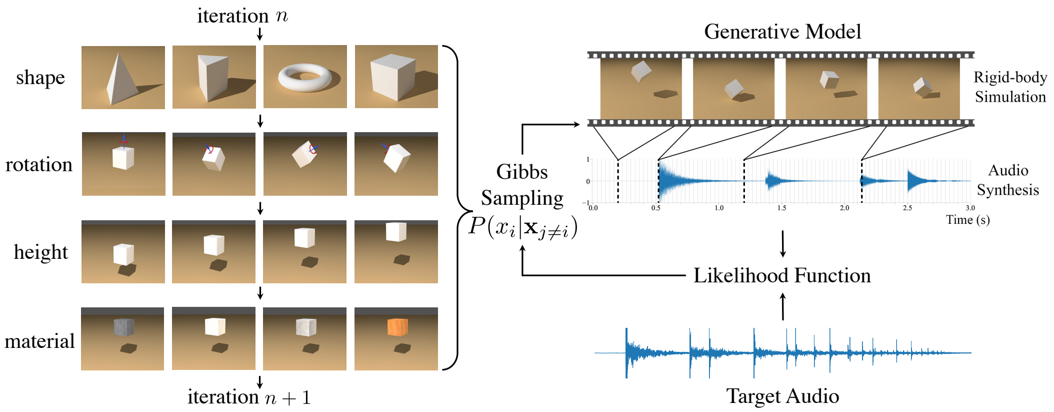

Figure 2: Our inference pipeline. We use Gibbs sampling over the latent variables. The conditional probability is approximated using the likelihood between reconstructed sound and the input sound.

Sound simulation Our sound synthesis engine builds upon and extends existing sound simulation systems in computer graphics and computer vision [O'Brien et al., 2001, 2002, James et al., 2006, Bonneel et al., 2008, Van den Doel and Pai, 1998, Zhang et al., 2017]. Van den Doel and Pai [1998] simulated object vibration using the finite element method and approximated the vibrating object as a single point source. O'Brien et al. [2001, 2002] used the Rayleigh method to approximate wave equation solutions for better synthesis quality. James et al. [2006] proposed to solve Helmholtz equations using the Boundary Element Method, where each object's vibration mode is approximated by a set of vibrating points. Recently, Zhang et al. [2017] built a framework for synthesizing large-scale audio-visual data. In this paper, we accelerate the framework by Zhang et al. [2017] to achieve near real-time rendering, and explore learning object representations from sound with the synthesis engine in the loop.

Physical Object Perception There has been a growing interest in understanding physical object properties like masses and frictions from visual input or scene dynamics [Chang et al., 2017, Battaglia et al., 2016, Wu et al., 2015, 2016, 2017]. Most of the existing research has been focusing on object properties from visual data. Recently, researchers started to explore learning object representations from sound. Owens et al. [2016a] attempted to infer material properties from audio, focusing on the scenario of hitting objects with a drumstick. Owens et al. [2016b] further demonstrated audio signals can be used as supervision on learning object concepts from visual data, and Aytar et al. [2016] proposed to learn sound representations from corresponding video frames. Zhang et al. [2017] discussed the complementary role of auditory and visual data in recovering both geometric and physical object properties. In this paper, we propose to learn physical object representations through a combination of powerful deep recognition models and analysis-by-synthesis inference methods.

Analysis-by-synthesis Our framework also relates to the field of analysis-by-synthesis, or generative models with data-driven proposals [Yuille and Kersten, 2006, Zhu and Mumford, 2007, Wu et al., 2015], as we are incorporating a graphics engine as a black-box synthesizer. Unlike earlier methods that focus mostly on explaining visual data, our work aims to infer latent parameters from auditory data. Please refer to Bever and Poeppel [2010] for a review of analysis-by-synthesis methods.

3 An Efficient, Physics-Based Audio Engine

At the core of our inference pipeline is an efficient audio synthesis engine. In this section, we first give a brief overview of existing synthesis engines, and then present our technical innovations on accelerating existing systems to real-time rendering for our inference algorithm.

3.1 Audio Synthesis Engine

Audio synthesis engines generate realistic sound by following fundamental physical laws. First, the interaction between an object and the environment is generated using rigid body simulation, where

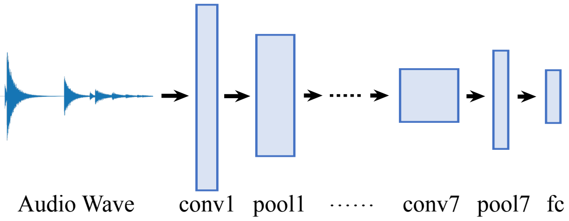

Figure 3: Our 1D deep convolutional network. Its architecture follows that in Aytar et al. [2016], where raw audio waves are forwarded through consecutive conv-pool layers, and then passed to a fully connected layer to produce output.

Settings	Time (s)
Original algorithm	30.4
Amplitude cutoff	24.5
Principal modes	12.7
Multi-threading	1.5
All	**0.8**

Table 1: Acceleration break down of each technique we adopted. Timing is evaluated by synthesizing an audio with 200 collisions. The last row reports the final timing after adopting all techniques.

Newton's physics laws dictate the object's motion and collisions over time. According to vibration analysis, each collision causes the object to vibrate in certain patterns, changing the air pressure around its surface. Such turbulence then propagates in air to the recording position and creates the sound of this physical process.

Rigid Body Simulation Given an object's 3D position and orientation and its mass and restitution, a physics engine can simulate the physical processes, and output the object's position, orientation, and collision information over time. In our implementation, an open-source physics engine, Bullet [Coumans, 2010], is used to simulate this process. In order to achieve accurate results, we use a time step of 1/300 second for the simulation. Specifically, we record the 3D pose and position of the object over time, as well as the collision locations, magnitudes, and directions. Object sound can then be approximated by accumulating sounds caused by those discrete impulse collisions on its surface.

Audio Synthesis The audio synthesis procedure is built upon previous work on simulating realistic sounds [James et al., 2006, Bonneel et al., 2008, O'Brien et al., 2001]. To facilitate fast synthesis, this process is decomposed into two parts: online and offline. The offline part first uses finite element method (FEM) to obtain the object's vibration modes, which depends on object's shape and its Young's modulus. The object vibration modes are then used as Neumann boundary conditions of the Helmholtz equation, which can be solved using boundary element method (BEM). The solution is then approximated using techniques reported by James et al. [2006], where the resulting pressure field is approximated by a sparse set of vibrating points. Note that the computation above only depends on object's shape and Young's modulus, but not on the physical process that it undergoes. This allows us to pre-compute a number of shape-modulus configurations before simulation; only minimal computation is needed at the simulation phase.

The online part of the audio engine loads pre-computed approximation and decomposes impulses on the surface mesh of the object onto its modal bases. Summing up pressure changes at the observation point induced by vibrations in each mode produces the desired sound. An evaluation of its authenticity can be found in Zhang et al. [2017].

3.2 Accelerating Audio Synthesis

The prerequisite for performing efficient inference via analysis-by-synthesis is fast audio synthesis. Unfortunately, the simulation procedure described above is expensive to compute. We therefore present ways for accelerating the computation to near real-time.

First, we pick out the most significant modes excited by each impulse. By setting a threshold at 90% energy cutoff, we shorten the computing time by ignoring sound components generated by insignificant modes, which are about one-half of total modes on average. Secondly, we stop synthesizing as the amplitude of the sound is damped below a small threshold, where humans can hardly perceive. Thirdly, we parallelize the synthesis process by treating each collision independently, which can be computed on an independent thread. We then join the completed threads into a shared buffer according to their time-stamps. The effect of acceleration is shown in Table 1. Online sound synthesis only contains variables that are fully decoupled from the offline stage, which enables us to freely manipulate other variables with little computational cost during simulation time.

Variable	Range	C/T	Variable	Range	C/T
Primitive shape (s)	14 classes	D	Specific modulus (E/ρ)	$[1, 30] \times 10^6$	D
Height (z)	$[1, 2]$	C	Restitution (e)	$[0.6, 0.9]$	C
Rotation axis (i, j, k)	S^2	C	Rotation angle (w)	$[-\pi, \pi)$	C
Rayleigh damping (α)	$10^{[-8,-5]}$	C	Rayleigh damping (β)	$2^{[0,5]}$	C

Table 2: Variables in our generative model, where the C/T column indicates whether sampling takes place in continuous (C) or discrete (D) domain, and values inside parentheses are the range we uniformly sampled from. Rotation is defined in quaternions.

3.3 Generating Stimuli

Because real audio recordings with rich labels are hard to acquire, we synthesize random audio clips using our physics-based simulation in order to test and evaluate our models. Specifically, we constrain ourselves only focusing on primitive objects falling onto the ground. We first construct a sound statistic data set that includes 14 primitives (partly shown in Table 2), each with 10 different specific moduli (defined as Young's modulus over density). With this pre-computed data, we are able to generate synthetic audio clips in a near-real-time fashion. Since the process of objects falling onto the ground is relatively fast, we set the total simulation time of each scenario to 3 seconds. An detailed synthesis setup can be found in Table 2.

4 Inference

In this section, we investigate four models for inferring object properties, each corresponding to a different scenario. We start from an unsupervised model where the input is only one single test case with no annotation. Inspired by how humans can infer scene information using a mental physics engine [Battaglia et al., 2013, Sanborn et al., 2013], we adopt Gibbs sampling over latent variables to find the combination that best reproduces the given audio. We develop this model further with the help from past experience, where a deep neural network is trained using data with inferred labels as supervision. Such self-supervised scheme is able to approximate the most probable configurations faster. We further investigate the case when labels can be acquired but are extremely coarse. We first train a recognition model with weak labels, then randomly pick candidates from those labels as an initialization for our analysis-by-synthesis inference. Lastly, in order to understand the limit for this inference task, we train a deep neural network with fully labeled data that yields the upper-bound performance.

4.1 Models

Unsupervised Given an audio clip S, we would like to recover all latent variables $\mathbf{x}$, so that the reproduced sound $g(\mathbf{x})$ is most similar to S. Suppose $L(\cdot, \cdot)$ is a likelihood function that measure the perceptual distance between two sounds, then the goal is to maximize $L(g(\mathbf{x}), S)$. We denote $L(g(\mathbf{x}), S)$ as $p(\mathbf{x})$ for brevity. In order to find $\mathbf{x}$ that maximizes $p(\mathbf{x})$, $p(\mathbf{x})$ can be treated as an distribution $\hat{p}(\mathbf{x})$ scaled with an unknown partition function Z. Since we do not have an exact form for $p(\cdot)$ nor $\hat{p}(\mathbf{x})$, Gibbs sampling is applied to draw samples from $p(\mathbf{x})$ using conditional probabilities. Specifically, at sweep round t, we update each variable $\mathbf{x}_i$ by drawing samples from

$$\hat{p}(x_i | x_1^t, x_2^t, ...x_{i-1}^t, x_{i+1}^{t-1}, ...x_n^{t-1}). \tag{1}$$

Such conditional probabilities, however, are much easier to approximate. For example, to sample Young's modulus conditioned on other variables, we could simply use the spectrogram as features, and measure the l_2 distance between two sounds, since Young's modulus would only affect the frequency at each collision. Under such observation, we use the spectrogram as features for all variables except height. Since the height can be inferred from the time of the first collision, a simple likelihood function can be designed as measuring the time difference between the first impact in two sounds. Note that this is only an approximate measure: object's shape and orientation also affects the time of the first impact. Nonetheless, since we are only concerned with conditional probabilities, such measure can be very effective.

To sample from the conditional probabilities, we adopt the Metropolis–Hastings algorithm, where samples are drawn from a Gaussian distribution and are accepted by flipping a biased coin according to its likelihood compared with the previous sample. Specifically, we calculate the l_2 distance d^t in feature space between $g(\mathbf{x}^t)$ and S. For a new sample $\mathbf{x}^{t+1}$, we also calculate the l_2 distance d^{t+1} in feature space between $g(\mathbf{x}^{t+1})$ and S. The new sample is accepted if d^{t+1} is smaller than d^t; otherwise, $\mathbf{x}^{t+1}$ is accepted with probability $\exp(-(d^{t+1} - d^t)/T)$, where T is a time varying function inspired by simulated annealing algorithm. In our implementation, T is set as a quadratic function of the current MCMC sweep number t.

Self-supervised Learning To accelerate the above sampling process we propose a self-supervised model, which is analogous to a Helmholtz machine trained by the wake-sleep algorithm. We first train a deep neural network, whose labels are generated by the unsupervised inference model suggested above for a limited number of iterations. For a new audio clip, our self-supervised model uses the result from neural network as an initialization, and then runs our analysis-by-synthesis algorithm to make further inference. By making use of past experience, the sampling process is expected to start off from a better position, and takes much fewer iterations to converge than the unsupervised model.

Weakly-supervised Learning We further investigate the case where weak supervision might be helpful for accelerating the inference process. Since the latent variables we aim to recover are hard to obtain in real world settings, it is more realistic to assume that we could acquire very coarse labels, such as the type of material, rough attributes of the object's shape, the height of the fall, *etc*. Based on such assumptions, we coarsen ground truth labels for all variables. For our primitive shapes, three attributes are defined, namely "with edge," "with curved surface," and "pointy." For material parameters, *i.e.*, specific modulus, Rayleigh damping coefficients and restitution, they are mapped to steel, ceramic, polystyrene and wood by finding the nearest neighbor to those real material parameters. Height is divided into "low" and "high" categories. A deep convolutional neural network is trained on our synthesized dataset with coarse labels. As shown in Figure 4, even trained using coarse labels, our network learns features very similar to the ones learned by the fully supervised network. To go beyond coarse labels, the unsupervised model is applied using the initialization suggested by the neural network.

Fully-supervised Learning To investigate the limit of this inference task, we train an oracle model with ground truth labels. To visualize what kind of abstraction and characteristic features are learned by oracle model, we plot inputs that maximally activate some hidden units in the last layer of the network. Figure 4 illustrates some of the most interesting waveforms. A selection of them learned to recognize specific temporal patterns, and others are most sensitive to specific frequencies. Similar patterns are found between weakly and fully supervised models.

4.2 Contrasting Model Performance

We would like to evaluate how well our model performs under different settings, especially on how past experience or coarse labeling could improve over the unsupervised model. We first present the implementation details of all four models, then compare their quantitative results on all inference tasks.

Sampling Setup We performed 80 sweeps of MCMC sampling over all the 7 latent variables; for every sweep, each variable is sampled twice. Shape, specific modulus and rotation are sampled by uniform distributions across their corresponding dimensions. For other continuous variables, we define an auxiliary Gaussian variable $x_i \sim \mathcal{N}(\mu_i, \sigma_i^2)$ for sampling, where the mean μ_i is based on current state. To evaluate the likelihood function between the input and the sampled audio (both with sample rate of 44.1k), we compute the spectrogram of the signal using Tuckey window of length 5,000 with a 2,000 sample overlap. For each window, a 10,000 point Fourier transform is applied.

Deep Learning Setup Our fully supervised and self-supervised recognition models inherit the architecture of SoundNet-8 [Aytar et al., 2016] as Figure 3, which takes an arbitrarily long raw audio wave as an input, and produces a 1024-dim feature vector. We append a fully connected layer at the

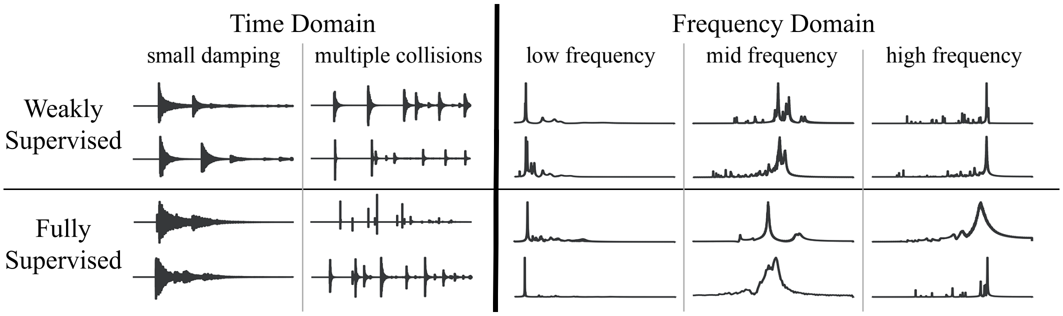

Figure 4: Visualization of top two sound waves that activate the hidden unit most significantly, in temporal and spectral domain. Their common characteristics can reflect the values of some latent variables, *e.g*. Rayleigh damping, restitution and specific modulus from left to right. Both weakly and fully supervised models capture similar features.

Inference Model		Latent Variables				
		shape	mod.	height	α	β
Unsupervised	init infer	8% 54%	10% 56%	0.179 0.003	0.144 0.069	0.161 0.173
Self-supervised	init infer	14% 52%	16% 62%	0.060 0.005	0.092 0.061	0.096 0.117
Weakly supervised	init infer	18% 62%	12% 66%	0.018 0.005	0.077 0.055	0.095 0.153
Fully supervised	infer	98%	100%	0.001	0.001	0.051

Table 3: Initial and final classification accuracies and label MSE errors of three different inference models after 80 iterations of MCMC, upper bounded by the fully supervised model.

end to produce a 28-dim vector as the final output of the neural network. The former 14 dimensions are the one-hot encoding of primitive shapes, the following 10 dimensions are encodings of the specific modulus. The last 4 dimensions regress the initial height, two Rayleigh damping coefficients and the restitution respectively. All the regression dimensions are normalized to a $[-1, 1]$ range. The weakly supervised model preserves the structure of fully supervised one, but with an 8-dim final output: 3 for shape attributes, 1 for height, and 4 for materials. We used stochastic gradient descent for training, with a learning rate of 0.001, a momentum of 0.9 and a batch size of 16. Mean Square Error(MSE) loss is used for back-propagation. We implemented our framework in Torch7 [Collobert et al., 2011], and trained all models from scratch.

Results Results for the four inference models proposed above are shown in Table 3. For shapes and specific modulus, we evaluate the results as classification accuracies; for height, Rayleigh damping coefficients, and restitution, results are evaluated as MSE. Before calculating MSE, we normalize values of each latent variable to $[-1, 1]$ interval, so that the MSE score is comparable across variables.

From Table 3, we can conclude that self-supervised and weakly supervised models provide better initialization for our analysis-by-synthesis algorithm, especially on the last four continuous latent variables. One can also observe that final inference accuracies and MSEs are marginally better than the unsupervised case. To illustrate the rate of convergence, we plot the likelihood value, $\exp(-kd)$ where d is the distance of sound features, along iterations of MCMC in Figure 5. The mean curve of self-supervised model meets our expectation, *i.e*., it converges much faster than the unsupervised model, and reaches a slightly higher likelihood at the end of 30 iterations. The fully supervised model, which is trained on 200,000 audios with the full set of ground-truth labels, yields near-perfect results for all latent variables.

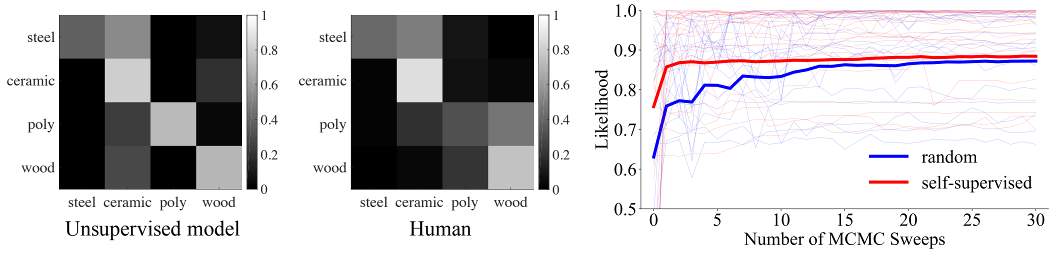

Figure 5: Left and middle: confusion matrix of material classification performed by human and our unsupervised model. Right: mean likelihood curve over MCMC iterations.

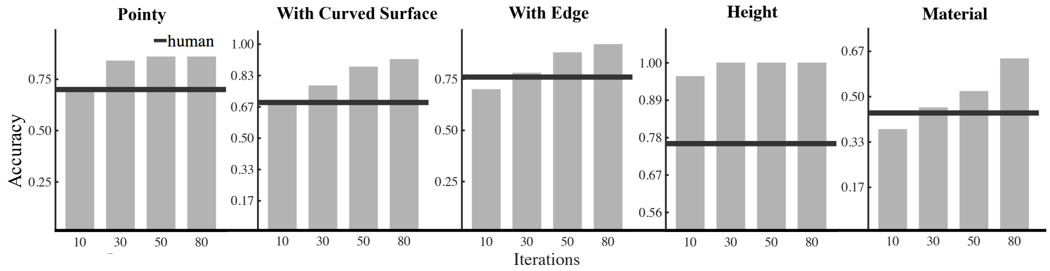

Figure 6: Human performance and unsupervised performance comparison. The horizontal line represents human performance for each task. Our algorithm closely matches human performance.

5 Evaluations

We first evaluate the performance of our inference procedure by comparing its performance with humans. The evaluation is conducted using synthetic audio with their ground truth labels. Then, we investigate whether our inference algorithm performs well on real-world recordings. Given an audio recorded under experiment settings, our algorithm is able to distinguish its shape among other candidates.

5.1 Human Studies

We try to understand how capable our inference model is relative to human performances. We designed three tasks on inferring object's shape, material and height of the fall, the most intuitive attributes when hearing object falling. Those tasks are designed to be classification problems, where the labels are in accordance with coarse labels used by our weakly-supervised model. The study was conducted on Amazon Mechanical Turk. For each experiment (shape, material, height), we randomly selected 52 test cases. Before answering test questions, the subject is shown 4 training examples with ground truths as familiarization of the setup. We collected 192 responses for the experiment on inferring shape, 566 for material, and 492 for height, resulting in a total of 1,250 responses.

Inferring Shapes After being familiarized with the experiment, participants are asked to make three binary judgments about the shape by listening to our synthesized audio clip. Prior examples are given for people to understand the distinctions of "with edge," "with curved surface," and "pointy" attributes. Due to material variations, humans mostly make those decisions based on temporal information rather than spectral information, *i.e.* the time sequence of collisions. As shown in Figure 6, humans are relatively good at recognizing shape attributes from sound and are around the same level of competency when the unsupervised algorithm runs for 10∼30 iterations.

Inferring Materials We sampled audio clips whose physical properties – density, Young's modulus and damping coefficients – are in the vicinity of true parameters of steel, ceramic, polystyrene and wood. Participants are required to choose one out of four possible materials. However, it can still be challenging to distinguish between materials, especially when sampled ones have similar damping

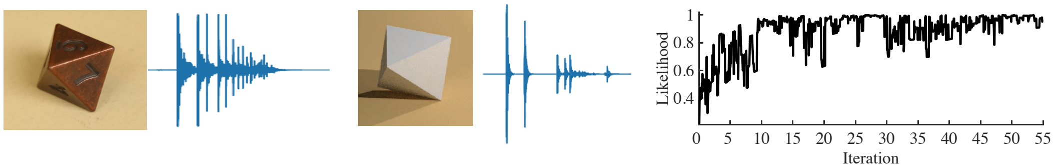

(a) Real shape and sound (b) Inferred shape and sound (c) Normalized likelihood over iterations

Figure 7: Results of inference on real world data. The test recording is made by dropping the metal dice in (a). Our inferred shape and reproduced sound is shown in (b). Likelihood over iteration is plotted in (c).

and specific modulus. Our algorithm confuses steel with ceramic and ceramic with polystyrene occasionally, which is in accordance with human performance, as shown in Figure 5.

Inferring Heights In this task, we ask participants to choose whether the object is dropped from a high position or a low one. We provided example videos and audios to help people anchor reference height. Under our scene setup, the touchdown times of the two extremes of the height range differ by 0.2s. To address the potential bias that algorithms may be better at exploiting falling time, we explicitly told humans that the silence at the beginning is informative. Second, we make sure that the anchoring example is always available during the test, which participants can always compare and refer to. Third, the participant has to play each test clip manually, and therefore has control over when the audio begins. Last, we tested on different object shapes. Because the time of first impact is shape-dependent, differently shaped objects dropped from the same height would have first impacts at different times, making it harder for the machine to exploit the cue.

5.2 Transferring to Real Scenes

In addition to the synthetic data, we designed real world experiments to test our unsupervised model. We select three candidate shapes: tetrahedron, octahedron, and dodecahedron. We record the sound a metal octahedron dropping on a table and used our unsupervised model to recover the latent variables. Because the real world scenarios may introduce highly complex factors that cannot be exactly modeled in our simulation, a more robust feature and a metric are needed. For every audio clip, we use its temporal energy distribution as the feature, which is derived from spectrogram. A window of 2,000 samples with a 1,500 sample overlap is used to calculate the energy distribution. Then, we use the earth mover's distance (EMD) [Rubner et al., 2000] as the metric, which is a natural choice for measuring distances between distributions.

The inference result is illustrated in Figure 7. Using the energy distribution with EMD distance measure, our generated sound aligns its energy at major collision events with the real audio, which greatly reduces ambiguities among the three candidate shapes. We also provide our normalized likelihood function overtime to show our sampling has converged to produce highly probable samples.

6 Conclusion

In this paper, we propose a novel model for estimating physical properties of objects from auditory inputs, by incorporating the feedback of an efficient audio synthesis engine in the loop. We demonstrate the possibility of accelerating inference with fast recognition models. We compare our model predictions with human responses on a variety of judgment tasks and demonstrate the correlation between human responses and model estimates. We also show that our model generalizes to constrained real data.

Acknowledgements

The authors would like to thank Changxi Zheng, Eitan Grinspun, and Josh H. McDermott for helpful discussions. This work is supported by NSF #1212849 and #1447476, ONR MURI N00014-16-1-2007, Toyota Research Institute, Samsung, Shell, and the Center for Brain, Minds and Machines (NSF STC award CCF-1231216).

References

Yusuf Aytar, Carl Vondrick, and Antonio Torralba. Soundnet: Learning sound representations from unlabeled video. In *NIPS*, 2016. 3, 4, 6

Peter W Battaglia, Jessica B Hamrick, and Joshua B Tenenbaum. Simulation as an engine of physical scene understanding. *PNAS*, 110(45):18327–18332, 2013. 1, 5

Peter W Battaglia, Razvan Pascanu, Matthew Lai, Danilo Rezende, and Koray Kavukcuoglu. Interaction networks for learning about objects, relations and physics. In *NIPS*, 2016. 3

Thomas G Bever and David Poeppel. Analysis by synthesis: a (re-) emerging program of research for language and vision. *Biolinguistics*, 4(2-3):174–200, 2010. 3

Nicolas Bonneel, George Drettakis, Nicolas Tsingos, Isabelle Viaud-Delmon, and Doug James. Fast modal sounds with scalable frequency-domain synthesis. *ACM TOG*, 27(3):24, 2008. 3, 4

Michael B Chang, Tomer Ullman, Antonio Torralba, and Joshua B Tenenbaum. A compositional object-based approach to learning physical dynamics. In *ICLR*, 2017. 3

Ronan Collobert, Koray Kavukcuoglu, and Clément Farabet. Torch7: A matlab-like environment for machine learning. In *BigLearn, NIPS Workshop*, 2011. 7

Erwin Coumans. Bullet physics engine. *Open Source Software: http://bulletphysics. org*, 2010. 4

Peter Dayan, Geoffrey E Hinton, Radford M Neal, and Richard S Zemel. The helmholtz machine. *Neural Comput.*, 7(5):889–904, 1995. 2

Doug L James, Jernej Barbič, and Dinesh K Pai. Precomputed acoustic transfer: output-sensitive, accurate sound generation for geometrically complex vibration sources. *ACM TOG*, 25(3):987–995, 2006. 3, 4

Roberta L Klatzky, Dinesh K Pai, and Eric P Krotkov. Perception of material from contact sounds. *Presence: Teleoperators and Virtual Environments*, 9(4):399–410, 2000. 2

Andrew J Kunkler-Peck and MT Turvey. Hearing shape. *J. Exp. Psychol. Hum. Percept. Perform.*, 26(1):279, 2000. 1, 2

Josh H McDermott, Michael Schemitsch, and Eero P Simoncelli. Summary statistics in auditory perception. *Nat. Neurosci.*, 16(4):493–498, 2013. 2

James F O'Brien, Perry R Cook, and Georg Essl. Synthesizing sounds from physically based motion. In *SIGGRAPH*, 2001. 3, 4

James F O'Brien, Chen Shen, and Christine M Gatchalian. Synthesizing sounds from rigid-body simulations. In *SCA*, 2002. 3

Andrew Owens, Phillip Isola, Josh McDermott, Antonio Torralba, Edward H Adelson, and William T Freeman. Visually indicated sounds. In *CVPR*, 2016a. 3

Andrew Owens, Jiajun Wu, Josh H McDermott, William T Freeman, and Antonio Torralba. Ambient sound provides supervision for visual learning. In *ECCV*, 2016b. 3

Davide Rocchesso and Federico Fontana. *The sounding object*. Mondo estremo, 2003. 2

Yossi Rubner, Carlo Tomasi, and Leonidas J Guibas. The earth mover's distance as a metric for image retrieval. *International journal of computer vision*, 40(2):99–121, 2000. 9

Adam N Sanborn, Vikash K Mansinghka, and Thomas L Griffiths. Reconciling intuitive physics and newtonian mechanics for colliding objects. *Psychol. Rev.*, 120(2):411, 2013. 1, 5

Max Siegel, Rachel Magid, Joshua B Tenenbaum, and Laura Schulz. Black boxes: Hypothesis testing via indirect perceptual evidence. In *CogSci*, 2014. 1, 2

Kees Van den Doel and Dinesh K Pai. The sounds of physical shapes. *Presence: Teleoperators and Virtual Environments*, 7(4):382–395, 1998. 3

Jiajun Wu, Ilker Yildirim, Joseph J Lim, William T Freeman, and Joshua B Tenenbaum. Galileo: Perceiving physical object properties by integrating a physics engine with deep learning. In *NIPS*, 2015. 3

Jiajun Wu, Joseph J Lim, Hongyi Zhang, Joshua B Tenenbaum, and William T Freeman. Physics 101: Learning physical object properties from unlabeled videos. In *BMVC*, 2016. 3

Jiajun Wu, Erika Lu, Pushmeet Kohli, William T Freeman, and Joshua B Tenenbaum. Learning to see physics via visual de-animation. In *NIPS*, 2017. 3

Alan Yuille and Daniel Kersten. Vision as bayesian inference: analysis by synthesis? *TiCS*, 10(7):301–308, 2006. 3

Zhoutong Zhang, Jiajun Wu, Qiujia Li, Zhengjia Huang, James Traer, Josh H. McDermott, Joshua B. Tenenbaum, and William T. Freeman. Generative modeling of audible shapes for object perception. In *ICCV*, 2017. 3, 4

Song-Chun Zhu and David Mumford. A stochastic grammar of images. *Foundations and Trends® in Computer Graphics and Vision*, 2(4):259–362, 2007. 3

Eberhard Zwicker and Hugo Fastl. *Psychoacoustics: Facts and models*, volume 22. Springer Science & Business Media, 2013. 1, 2